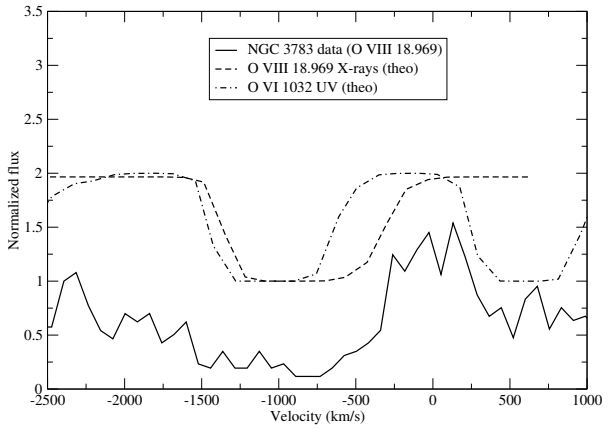

Fig. 12. Possible kinematical relationship between the UV and the X-ray absorbers. In the figure are plotted the theoretical X-ray and UV lines O VIII λ18.969 and O VI λ1032, dashed and short-dotted lines respectively. Also plotted is the profile of the line O VIII λ18.969 taken from the 900 ks spectrum of NGC 3783. All these lines are sharing velocities $\sim$1000 km s^{-1}.

5.3. *Present single wind vs multiphase wind scenario*

However, we want to highlight the most important differences between our model, consisting of a single wind governed by the laws of radiative acceleration, and the multiphase wind subjected to pressure equilibrium.

The first difference is that in our model there is a clear correlation between ionization state of the ions and velocity ($\xi - v$), and ξ and number of particle n_H ($\xi - n_H$). At the same time, because of the dependence of v and n_H on the spatial distance r, there is a dependence of ξ on r. This is different from the multicomponent in pressure equilibrium model, suggested by Netzer et al. (2003). In that model three components (in ionization) may coexist in the same volume of space and lie on the stable regions of the nearly vertical part of the thermal stability curve (log T *vs* log $[U/T]$, see Figure 12 in that paper). Our absorbers are not embedded in an external medium, and they cannot coexist at exactly the same location, but rather follow the physical laws of radiative acceleration. In this context, Gabel et al. (2005) also find that the UV absorbers of NGC 3783 may share some properties of the multiphase thermal wind. The UV kinematic components 1b, 2 and 3 could occupy the low-temperature base of the region of the thermal stability curve where a range of temperatures can coexist in pressure equilibrium. There is one weak point in the picture of inhomogeneities coexisting in pressure equilibrium. The low-ionization high-velocity UV absorber does not fit there, due to a pressure of a factor of 10 larger than that of the other component. If embedded into a more ionized-hotter material, it will eventually evaporate, unless there exists an additional confining mechanism. This extra confinement could be provided by magnetic pressure, requiring moderate magnetic fields ($B \approx 10^{-3}$ G), as predicted by some dynamical models (Emmering, Blandford, & Shlosman 1992; de Kool & Begelman 1995). In our model, there is no need for a confining mechanism, and if anything, the more ionized material is closer to the source, shielding the intense continuum radiation and preventing its evaporation. We conclude by stating that our model represents an additional competitor. It cannot be ruled out by comparison with the pressure equilibrium model. A more detailed comparison between models is beyond the scope of the present work, but could take place in the future.

6. TWO OUTFLOWS

So far we have been concerned with the line velocity shifts as measured with respect to the points of maximum absorption of the lines, but little has been said about the asymmetry of the troughs. To quantify the line asymmetries predicted by the theoretical models we have tabulated the fraction of the terminal velocity at which the absorption is maximum, to be compared with the ratio ($\bar{v}/v_1$), where v_1 is the position of the blue edge of each line, used to quantify the asymmetry in the spectrum of NGC 3783 (see Table 3 Ramírez et al. 2005). We characterize a theoretical line as "red" if $v(\tau_{\max})/v_\infty > 0.5$ and as "blue" if $v(\tau_{\max})/v_\infty < 0.5$, while for observed lines they are grouped according to $\bar{v}/v_1 > 0.5$ and $\bar{v}/v_1 < 0.5$ (see Ramírez et al. 2005). In Table 3 we present the observed troughs. In the first and second columns are given the identifications and the wavelengths of the lines, in the third, the fraction $v(\tau_{\max})/v_\infty$ for model A, and in the fourth the classification from observed lines, as in Ramírez et al. (2005), i.e., $\bar{v}/v_1$. We classify every trough as either (R) if it is red or (B) if it is blue. There are clear discrepancies between model A and the observations. In order to improve the agreement with observations we found it necessary to create a model composed of two outflows, which differ by their log ξ_0, the initial exposition to the source. In Table 4 we can see separately the parameters of the two outflows which compose model C. The first flow, with $\log \xi_0 = 3$, which we call HIF (high ionization flow), is able to create the majority of the high ionization lines (S XVI λ4.729, S XV λ5.039, Fe XXIII λ8.303), with